Molecular Vision 2025; 31:160-173 <http://www.molvis.org/molvis/v31/160>
Received 16 August 2024 | Accepted 8 April 2025 | Published 10 April 2025

Inhibitory effects of ursolic acid on oxygen-induced mouse retinal neovascularization via intravitreal injection

Lu Yang,[1,2,3,4] Fen Yang,[5] Weiliang Zhang,[6] Yanhua Wang,[3] Peng Chen,[3] Shufang Du,[5] Xiaoyan Liu,[5] Yan Gao,[4] Junhua Shi,[4] Peng Wang,[3] Rui Li,[3] Qiang Su[7]

(The first three authors contributed equally to this study)

[1]Department of Ophthalmology, Aier Eye Hospital, Jinan University, Hainan Aier New Hope Eye Hospital, Haikou, Hainan, China; [2]Department of Ophthalmology, Aier Eye Hospital, Jinan University, Guangzhou, Guangdong, China.; [3]Department of Ophthalmology, Shanxi Aier Eye Hospital, Taiyuan, Shanxi, China; [4]Department of Ophthalmology, Taiyuan Aier Eye Hospital, Taiyuan, Shanxi, China; [5]Department of Ophthalmology, Shanxi Eye Hospital, Taiyuan, Shanxi, China; [6]Department of Ophthalmology, Shanxi Bethune Hospital, Taiyuan, Shanxi, China; [7]Department of Ophthalmology, The First Hospital of Shanxi Medical University, Taiyuan, Shanxi, China

Objective: This study aimed to explore the effects and mechanisms of ursolic acid (UA) on oxygen-induced retinal neovascularization (RNV) in mice and its inhibitory effects on human retinal capillary endothelial cells (HRCECs) under high-glucose conditions.

Methods: Neonatal mice were divided into five groups: one normal group and four with oxygen-induced retinopathy (OIR), including OIR, phosphate-buffered saline, UA and Lucentis groups. On postnatal day 17 (P17), mice were euthanized and one eye was collected for retinal analysis using fluorescence microscopy. Protein and messenger ribonucleic acid (mRNA) levels of vascular endothelial growth factor (VEGF), matrix metalloproteinase (MMP)-2, MMP-9 and cyclo-oxygenase-2 (COX-2) were detected. HRCECs cultured under high-glucose conditions were treated with UA to assess its effects on proliferation and molecular expression.

Results: UA significantly reduced RNV area in OIR mice and protected astrocytes from hypoxia-induced damage ($p<0.01$). VEGF, MMP-2, MMP-9 and COX-2 levels were lower in the UA group compared with the OIR and phosphate-buffered saline groups ($p<0.05$), but slightly higher than in normal controls ($p<0.01$). Lucentis reduced VEGF levels but did not significantly affect MMP-2, MMP-9 or COX-2. In HRCECs, UA inhibited high-glucose-induced proliferation and reduced VEGF, MMP-2, MMP-9 and COX-2 expression in a time- and dose-dependent manner.

Conclusions: UA inhibits RNV by reducing VEGF, MMP-2, MMP-9 and COX-2 expression, protecting astrocytes and suppressing HRCEC proliferation under high-glucose conditions, highlighting its therapeutic potential for retinal neovascular diseases.

Retinal neovascularization (RNV)-related diseases are a type of pathology with various causes [1]. The condition's pathological changes [2] include vascular proliferation accompanied by bleeding, exudation and the formation of an organic fibrous membrane, eventually leading to visual loss. It is one of the most serious blinding eye diseases [3] and includes retinopathy of prematurity (ROP), proliferative diabetic retinopathy (DR) and retinal (central/branch) vein obstruction [1]. RNV is the basis of the pathologic change, which is why its effective inhibition is particularly important. Numerous studies on retinal neovascular proliferative diseases have focused on vascular damage in RNV formation. Therefore, it is necessary to develop new drugs that can effectively inhibit RNV in clinical work. Studies have confirmed that vascular endothelial growth factor (VEGF), cytokine matrix metalloproteinase (MMP)-2, MMP-9 and cyclo-oxygenase-2 (COX-2) [4] are key factors in angiogenesis.

Currently, anti-VEGF agents, such as ranibizumab (Lucentis), are widely used in clinical practice for RNV-related diseases and have demonstrated significant efficacy in reducing neovascularization. However, these treatments have limitations, including the need for repeated intravitreal injections and the potential for adverse effects, such as inflammation and endophthalmitis. Therefore, there is a pressing need to explore alternative therapeutic agents with fewer side effects and potentially broader mechanisms of action.

Ursolic acid (UA), a natural pentacyclic triterpenoid found in many medicinal plants, has garnered attention for its diverse pharmacological properties. Chemically, UA comprises a hydroxyl group at the C-3 position, a carboxyl group at C-17 and a hydrophobic pentacyclic structure,

Correspondence to: Lu Yang, Department of Ophthalmology, Aier Eye Hospital, Jinan University, Hainan Aier New Hope Eye Hospital, Haikou, Hainan, China; No.165 Fengxiang East Road, Qiongshan District, Haikou, Hainan , China; 571100,Phone: +86-0898-65727580; email: yl16082022@163.com

contributing to its lipophilic nature and biologic activity. Its bioactivities include anti-inflammatory, antioxidant, anticancer and cardioprotective effects. In ophthalmology, UA has emerged as a potential therapeutic agent due to its ability to regulate angiogenesis, reduce oxidative stress and inhibit inflammatory pathways. Previous studies have shown that UA can inhibit tumor angiogenesis by targeting multiple proangiogenic factors, including VEGF, MMPs and COX-2 [5]. UA also possesses anti-inflammatory and antioxidant properties, further enhancing its therapeutic potential in various diseases. Beyond its anticancer effects, UA has demonstrated cardioprotective properties, including the mitigation of oxidative stress and the prevention of doxorubicin-induced cardiac damage [6]. These findings suggest that UA may regulate angiogenesis and improve vascular stability through multiple pathways, making it a promising candidate for the treatment of RNV-related diseases.

However, the role of UA in RNV has, to date, rarely been studied. This study investigates whether UA can inhibit RNV and thus impact RNV in mice with oxygen-induced retinopathy (OIR).

METHODS

Animal models and treatment: A total of 75 healthy seven-day-old (P7) specific pathogen-free-grade C57BL/6J mice with a body mass of 4.59 ± 0.57 g were used for this research (regardless of sex). The study animals were purchased from the Laboratory Animal Centre of Shanxi Medical University, China. All animal experiments were approved by the Animal Ethics Committee of the Shanxi Aier Eye Hospital.

The specific treatment methods are follows: For OIR animal modeling, 60 healthy clean-grade C57BL/6J mice on P7 were placed into feeder oxygen tanks with female mice and connected to 100% medical moist pure oxygen with oxygen flow at approximately 1 l/min [7]. The oxygen concentration was regulated and monitored with an oxygen controller at 75% ± 3% and room temperature (23 °C ± 2 °C). Lighting was normal fluorescent light, with a day-night cycle of 12 h:12 h. The mice were observed every second day. Between observation days, the oxygen tanks were opened promptly to perform necessary maintenance operations but no medicine injections were administered to the mice during this period. Additionally, the female mice were replaced along with pad materials, feeding and water. The mice were housed under high-oxygen partial pressure for five days and removed from the oxygen tank on P12.

In the normal control group, 15 newborn mice were kept in a 23 °C ± 2 °C tank with normal air (without oxygen). The mice in all groups were kept in a tank with 23 °C ± 2 °C normal air for five days until P17.

The successfully modeled OIR mice were randomly divided into four groups: OIR group, phosphate-buffered saline (PBS) group, UA group and Lucentis group (positive control group; n=15, each). On P12–P16, 3 µl PBS buffer (PBS group), 3 µl UA (2 g/l; solid powder, purity >90%; Sigm-Aldrich, St. Louis, MO; UA group) and 3 µl Lucentis injection (Novartis, Basel, Switzerland; Lucentis group) were injected into the vitreous cavity of the mice [8,9]. The normal group and the OIR group were not treated.

Sample collection: Sample size (n=75) was determined based on our previous studies to ensure sufficient statistical power. A minimum of 15 mice per group was selected, allowing for adequate biologic replicates while accommodating potential variability in experimental outcomes. On P17 the mice were euthanized via anesthesia using 1.0% sodium pentobarbital (80 mg/kg, 100,203, Xi'an Guoan Biotechnology Co., Ltd., China). One eye was removed from each mouse for retinal flat-mount preparation and *Griffonia simplicifolia* type I lectin, isolectin B4 (GS-IB4) fluorescence staining. The RNV area and central retina were analyzed using Image-Pro Plus (v.5.1, Media Cybernetics, Rockville, MD) software. The contralateral eyeballs were removed, and retinal tissue was extracted under sterile conditions and immediately stored in liquid nitrogen for western blot and real-time PCR analyses to test for VEGF, MMP-2, MMP-9 and COX-2.

Culture and identification of human retinal capillary endothelial cells: For human retinal capillary endothelial cell (HRCEC) culture, one to two donor eyeballs were obtained per session in a sterile operating room following corneal transplantation. The donor eyeballs were derived from the post-surgical remains of human corneal transplants, ensuring compliance with ethical guidelines and sterility during handling. The eyeballs were carefully incised along the equator under sterile conditions. Using a dissection microscope, the vitreous vessels and membranes of the retina were carefully stripped using micro-instruments, ensuring that the integrity of the retinal cells was preserved. This procedure specifically targeted the removal of vitreous components rather than the retinal nerve fiber layer. The dissected tissue was enzymatically digested using 0.25% trypsin-EDTA at 37 °C for 15 min with intermittent agitation to dissociate the cells. After digestion, the suspension was mechanically fragmented, homogenized and filtered through a 70-µm mesh to remove tissue debris. The enzymatic reaction was terminated by adding 10% fetal bovine serum. The cell suspension was centrifuged at 300 ×g for five min to collect the cells, which were then resuspended in a complete human endothelial cell

culture medium (10% fetal bovine serum, 100 µ/ml penicillin, 50 µ/ml gentamicin; #M200500, Gibco, Grand Island, NY). Cells were seeded into culture flasks and incubated in a humidified 5% CO_2 incubator at 37 °C. The fluid was changed according to the cell growth rate approximately once every one to two days. During culture, retinal vascular endothelial cells were morphologically assessed by flattening, and any cobblestone morphology was noted. To prevent interference from red blood cells in the observation and analysis of endothelial cells, as well as to avoid the effects of glial cells on the growth, proliferation and differentiation of endothelial cells, these contaminating cells were carefully removed to ensure accurate experimental results. Miscellaneous cell locations were marked microscopically, and miscellaneous cells, such as red blood cells and glial cells, were removed using cell scraping. Primary cells in the culture vial were subcultured if the adherent area was >80% [10].

For the identification of HRCECs, their growth characteristics and morphological characteristics were observed using an inverted phase-contrast microscope. Cells were assessed for cobblestone morphology, indicating endothelial cell integrity and purity. Cells in good growth condition were used to prepare a suspension at a concentration of approximately 4.5×10^4 cells/ml. Sterile coverslips were placed in a 24-well plate, inoculated with 1 mL of suspension per well and cultured in an incubator. After the cells were evenly distributed on the slides, they were washed twice with PBS, followed by fixation with 4% paraformaldehyde for 30 min. They were subsequently rinsed three times with PBS. Factor VIII-related antigen-antibody was added to confirm endothelial cell identity, and the cells were incubated overnight at 4 °C. After washing, a secondary antibody conjugated with a fluorescent marker was applied, followed by additional PBS rinses. Cells were observed under a fluorescence microscope for antigen expression. Images were captured to document the characteristic features of HRCECs, validating their endothelial nature.

Measurement of retinal pathological neovascularization, nonperfusion area and morphological observation of astrocytes: Mice were taken at the corresponding time points and euthanized via anesthesia. The eyes were carefully removed, fixed in 4% paraformaldehyde (40 min or four hours on ice) and slowly washed for 20 min four times in a PBS liquid shaker (Eppendorf, Hamburg, Germany). A corneal bayonet puncture was performed in the anterior chamber and the anterior eye segment was removed by cutting the eye equator at the angular scleral rim. Then, the retina was carefully dissected and the cohesive vitreous tissue was removed as cleanly as possible. The retina was stained with Isolectin GS-IB4 (1:50; Sigma-Aldrich), glial fibrillary acidic protein (1:50; Sigma-Aldrich) and 4’,6-diamidino-2-phenylindole (1:500; Sigma-Aldrich) at 4 °C overnight, with 25 µl per eyeball. After cutting the radial four-flap of the eye cup, it was neatly tiled on a slide and sealed using an antifluorescence attenuation sealing tablet. The morphology and distribution of RNV and the ischemic nonperfusion area were observed under a fluorescence microscope (×50, 500-µm scale; Leica Microsystems, Wetzlar, Germany) and the relative area of RNV and the ischemic avascular area (proportion of total retinal area) were measured using Image-Pro Plus software (Media Cybernetics). The subtle morphology and distribution of RNV (IB4-positive) and astrocytes (glial fibrillary acidic protein-positive) were observed under a confocal microscope (×400, 100-µm scale; Zeiss, Oberkochen, Germany).

Human retinal capillary endothelial cell proliferation measured with methyl thiazolyl tetrazolium assay: Cells that were well cultured were harvested and the supernatant was removed. Subsequently, 1.0 mL high-glucose culture medium (human endothelial cell culture medium [Gibco, catalog #11965–092] supplemented with 30 mmol/l glucose) and 1.0 ml of normal glucose culture medium (human endothelial cell culture medium [Gibco, catalog #11885–084] supplemented with 5 mmol/l glucose) were added. The cells were then seeded into 96-well plates at a density of approximately 5×10^3 cells per well, with a total volume of 200 µl per well. This experiment comprised six groups, each containing five replicate wells.

Cell experiment groups: (1) treatment normal glucose (TN) group—normal glucose (glucose concentration, 5.5 mmol/l); and (2) the treatment high-glucose (TH) group—high glucose (glucose concentration, 25 mmol/l) [11]. T1 group—high glucose + 5 µmol/l UA; T2 group—high glucose + 10 µmol/l UA; T3 group—high glucose + 20 µmol/l UA; and T4 group—high glucose + 40 µmol/l UA. The marginal wells of the 96-well plate were only filled with culture medium as a blank control for trimming and evaporation and the culture medium was discarded when cells were adherent. The UA stock solution was then prepared and diluted with a high-glucose medium to achieve the desired concentration, which was subsequently added according to the experimental grouping. In the TN group, 200 µl normal glucose culture medium was added to each well; in the TH group, 200 µl high-glucose culture medium was added to each well. For the T1–T4 groups, diluted UA solution was added to 96-well plates at 200 µl/well according to a UA concentration of 5, 10, 20 and 40 mol/l, respectively. The cells were incubated for 24, 48 and 72 h, respectively, and then 20 µL of a methyl thiazolyl tetrazolium powder solution was added to each well

and cultured for 4 h. After discarding the culture medium, the cells were washed three times with PBS. Then, 20 µl of a dimethyl sulfoxide solution was added to each well and shaken for 10 min until its blue–purple crystal was dissolved. The 96-well plate was placed inside the plate reader (BioTek ELx800, BioTek Instruments, Inc., Winooski, VT) with a selected wavelength of 490 nm and the results were calculated according to the following formula: cell survival rate = average optical density (OD) of the experiment groups (T1–T4) / average OD of the control groups (TN, TH) × 100%; cell inhibition rate = (1 − OD in the experiment groups / OD in the control groups) × 100%. All of the above steps were repeated three times to calculate the final results.

Protein expression of vascular endothelial growth factor, matrix metalloproteinase-2, matrix metalloproteinase-9 and cyclo-oxygenase-2 in the retinal tissue samples detected using western blot analysis: The total protein was extracted from each group of tissue samples using a lysis buffer (Sigma-Aldrich) and the protein supernatant was quantified for protein concentration. The level of protein was quantitated using a bicinchoninic acid assay kit (Sigma-Aldrich). A 10% sodium dodecyl sulfate polyacrylamide gel electrophoresis gel and sample protein were prepared in each well (the total protein in each well was equal based on the protein concentration). Electrophoresis was performed using an electrophoresis instrument and transmembrane transfer was performed using gel transfer apparatus. Subsequently, sodium dodecyl sulfate polyacrylamide gel electrophoresis was adopted to separate the protein lysates and moved to polyvinylidene fluoride membranes (Invitrogen, Carlsbad, CA). The protein was blocked in 5% nonfat milk powder for one to two hours and washed three to four times with PBS (Sigma-Aldrich). Samples were incubated with 1‰ VEGF (Abcam, Cambridge, MA), MMP-9 (Abcam) and COX-2 antibodies (Abcam) and monoclonal mouse anti-β-actin antibody (Cell Signaling Technology, Danvers, MA) as an internal control at 4 °C overnight. The samples were then washed three times with PBS before adding the corresponding secondary antibodies (Abcam), incubated for one hour at room temperature and washed three to four times with PBS. After membrane washing, the sample silicon film was exposed using an electrochemiluminescence kit (Sigma-Aldrich). Gray band values were analyzed using ImageJ software (National Institutes of Health, Bethesda, MD). The experiments were repeated three times.

Messenger ribonucleic acid expression of vascular endothelial growth factor, matrix metalloproteinase-2, matrix metalloproteinase-9 and cyclo-oxygenase-2 in retinal tissue determined using real-time polymerase chain reaction: Total ribonucleic acid (RNA) from each tissue was extracted using TRIzol Reagent (Takara, Tokyo, Japan) and tested for purity and concentration using an ultraviolet spectrophotometer. Reverse transcription reactions were performed using a reverse transcription kit; PCR was performed using the fluorescence quantitative PCR kit (DRR036A Takara PCR Amplification Kit); all PCRs were performed using the indicated PCR instrument. Glyceraldehyde triphosphate dehydrogenase was used as the internal reference to calculate the relative quantification values ($2^{-\square\square Ct}$). The specific primer sequences for VEGF, MMP-2, MMP-9, COX-2 and glyceraldehyde 3-phosphate dehydrogenase (Shanghai Sangon Biotechnology Company, Shanghai, China) are detailed in Table l.

Statistical methods: Statistical analysis was processed using SPSS (v.18.0) software (IBM, Armonk, NY) and measurement data were expressed as mean ± standard deviation. The data of each sample were normally distributed (analyzed using the Kolmogorov–Smirnov method), and homogeneity of variance testing confirmed the homogeneity of variance (using the Levene test). The relative protein expression ratio (gray band value) and mRNA expression ratio (relative quantification value) between the experiment and control groups were compared using a one-way ANOVA, and the least significant difference Student *t* test was used for multiple comparisons between groups; $p<0.05$ indicated a statistically significant difference.

RESULTS

Hypoxic-phase injection of ursolic acid significantly reduced retinal neovascularization cluster formation and accelerated physiologic vascular reconstruction in mice with oxygen-induced retinopathy: According to immunofluorescence staining of the retinal flat mounts of the P17 mice, when UA was injected at P12–P16 (hypoxia) in the C57BL/6J mice the retinal veins in the OIR and PBS groups were relatively beaded, with a large central avascular perfusion area and a large number of highly fluorescence-stained neovascular groups were visible on the periphery when compared with the normal group. There was no statistical difference between the OIR group and the PBS group. Compared with the OIR group, the retinal neovascular area decreased by 75.4% and 76.5% in the UA and Lucentis groups, respectively (t=8.79, 7.28; all $p<0.01$), whereas the nonperfusion area decreased by 73.3% and 74.1% in the UA and Lucentis groups, respectively (t=8.17, 7.44; all $p<0.01$). However, there was no statistical difference between the UA group and the Lucentis group (Figure 1).

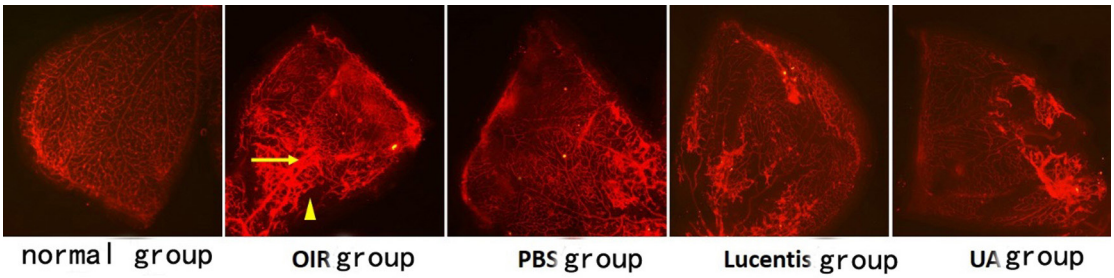

Figure 1. Retinal neovascularization and formation of nonperfusion areas in each group. Compared with the normal group, the retinal veins in the oxygen-induced retinopathy group are beaded, with a large avascular perfusion area in the center (triangle) and a large number of highly fluorescent stained neovascularization groups are visible in the surrounding area (arrow).

Hypoxic-phase injection of ursolic acid morphologically reduced the formation of retinal neovascularization clusters in mice with oxygen-induced retinopathy and alleviated hypoxia-induced damage to retinal astrocytes: According to the confocal microscopy results of the retinal flat mounts of P17 mice in each group, the degree of neovascularization in the OIR and PBS groups was significantly increased, and the shape was polyneoplastic and massive when compared with the normal group. Neovascularization not only proliferated in the same plane but also protruded into the vitreous cavity, forming the mass accumulation of neovascularization. Astrocytes were primarily (or even entirely) heteromorphic and cell body arrangement was more disordered as the astrocytes had lost their normal stellate and dendritic shape. In the UA and Lucentis groups, the proliferation of neovascularization was not significant and lacked significant polytumors and large mass accumulations compared with the OIR group. Neovascularization was isolated or proliferated only within the same plane and rarely protruded into the vitreous cavity. The morphology and cell arrangement of astrocytes closely resembled normal stellate and dendritic morphology, with few heteromorphic parts (Figure 2).

Expression of vascular endothelial growth factor, matrix metalloproteinase-2, matrix metalloproteinase-9 and cyclo-oxygenase-2 proteins in the retinal tissue samples of each group: VEGF protein expression was significantly higher in the OIR and PBS groups than in the UA, Lucentis and normal groups, with significant statistical differences ($p<0.05$); however, there was no significant difference between the OIR and PBS groups ($p>0.05$). VEGF protein expression in the UA and Lucentis groups was slightly higher than in the normal

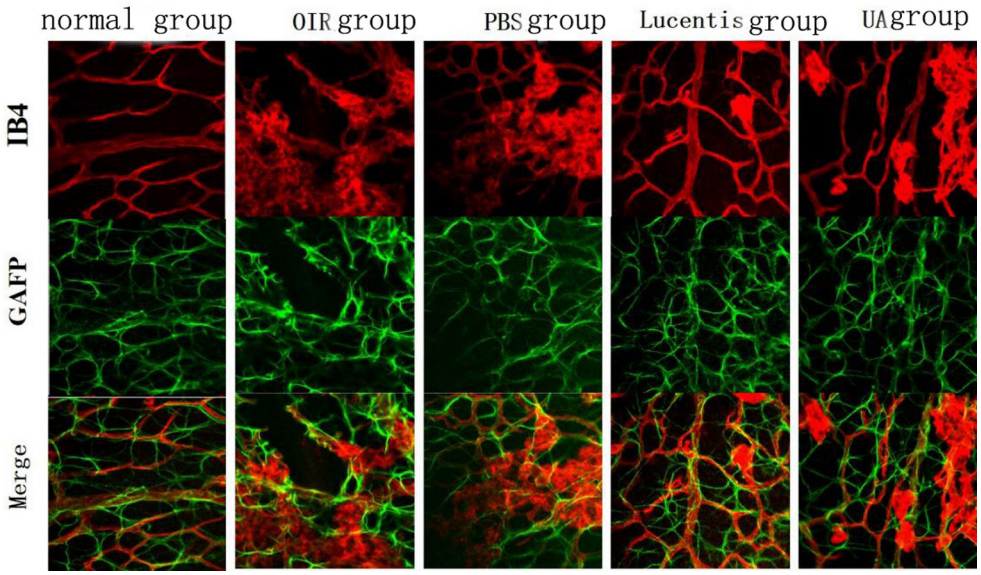

Figure 2. Retinal neovascularization and astrocyte morphology in mice in each isolectin B4 group (red, neovascularization staining); glial fibrillary acidic protein (green, astrocytes staining); merge.

group; the difference was statistically significant (p<0.05). However, there was no significant difference between the UA and Lucentis groups (p>0.05; Figure 3A). Protein expression of MMP-2, MMP-9 and COX-2 was significantly higher in the OIR, PBS and Lucentis groups than in the UA and normal groups; the difference was statistically significant (p<0.05). However, there was no significant difference between the OIR, PBS and Lucentis groups (p>0.05). Protein expression of MMP-2, MMP-9 and COX-2 was slightly higher in the UA group than in the normal group; the difference was statistically significant (p<0.05; Figure 3B–D).

Vascular endothelial growth factor, matrix metalloproteinase-2, matrix metalloproteinase-9 and cyclo-oxygenase-2 messenger ribonucleic acid levels in the retinal tissue samples of each group: VEGF mRNA levels were significantly higher in the OIR and PBS groups than in the UA, Lucentis and normal groups (p<0.05); however, there was no significant difference between the OIR group and the PBS group (p>0.05). VEGF mRNA levels were slightly higher in the UA and Lucentis groups than in the normal group; the difference was statistically significant (p<0.05). However, there was no significant difference between the UA and Lucentis groups (p>0.05; Figure 4A).

MMP-2, MMP-9 and COX-2 mRNA levels were significantly higher in the OIR, PBS and Lucentis groups than in the UA group and the normal group; the difference was statistically significant (p<0.05). However, there was no significant difference among the OIR, PBS and Lucentis groups (p>0.05). MMP-2, MMP-9 and COX-2 mRNA levels were slightly higher in the UA group than in the normal group; the difference was statistically significant (p<0.05; Figure 4B–D).

Effect of different concentrations of ursolic acid on human retinal capillary endothelial cell proliferation in a high-glucose environment: The HRCECs were seeded in 96-well plates. During the same culture period, the number of HRCECs in the normal glucose group was small compared with the high-glucose group (p<0.05). After 24, 48 and 72 h

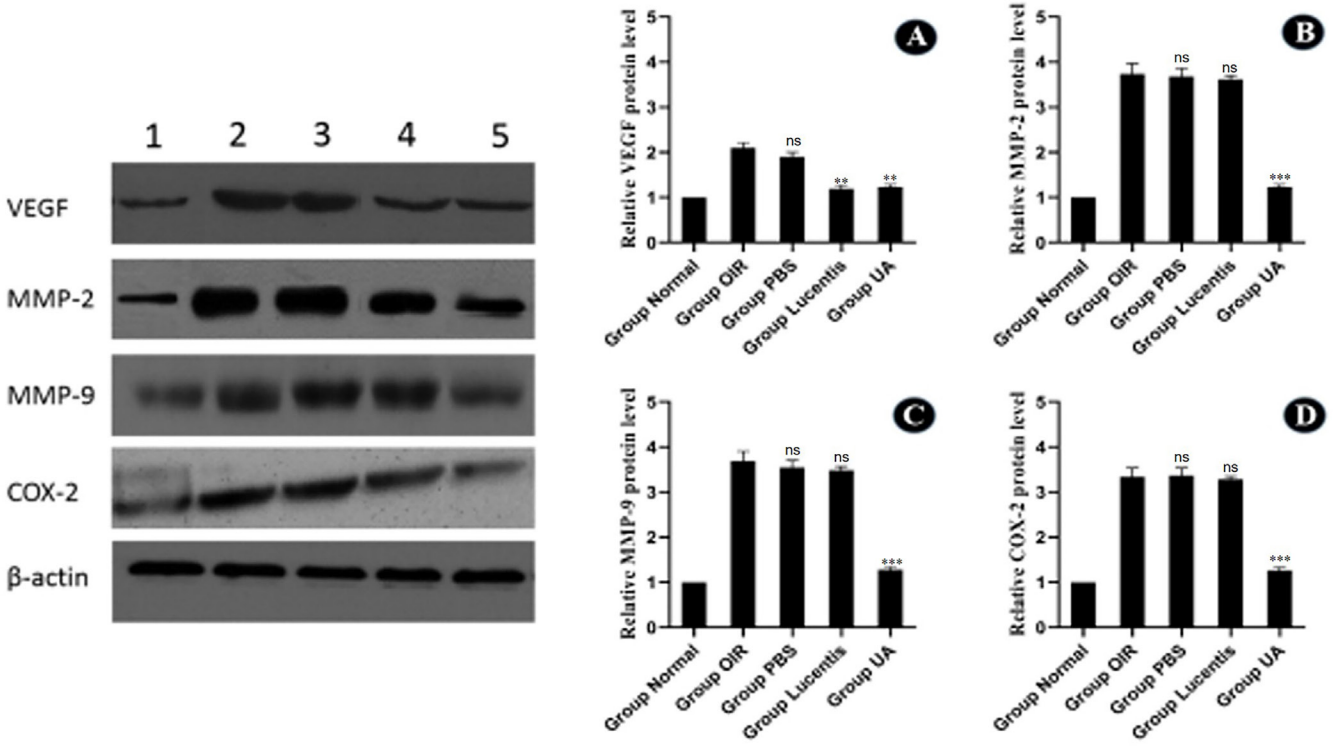

Figure 3. Expression of various proteins. Expression levels of vascular endothelial growth factor (**A**), matrix metalloproteinase 2 (**B**), matrix metalloproteinase 9 (**C**) and cyclo-oxygenase 2 (**D**) proteins in the retinal tissues of all groups: 1. Normal group; 2. oxygen-induced retinopathy (OIR) group; 3. phosphate-buffered saline group; 4. Lucentis group; 5. ursolic acid group. VEGF: vascular endothelial growth factor; MMP-2: Matrix metalloproteinase 2; MMP-9: Matrix metalloproteinase 9; COX-2: Cyclo-oxygenase 2; UA: Ursolic acid; ns: Not significant; **p<0.01 compared with OIR group; ***p<0.001 compared with OIR group.

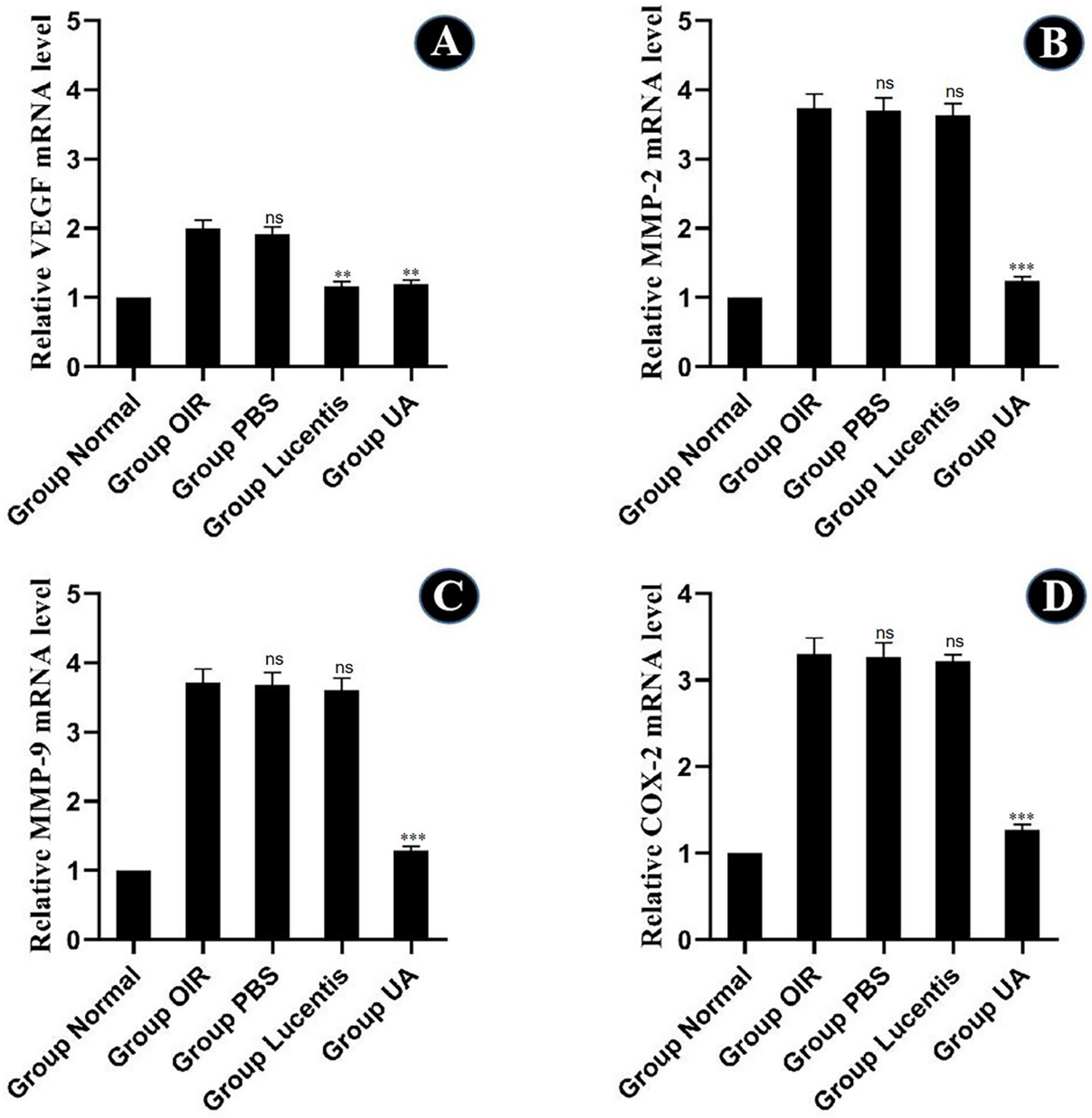

Figure 4. The mRNA expression of genes in each group. Expression levels of vascular endothelial growth factor (**A**), matrix metalloproteinase 2 (**B**), matrix metalloproteinase 99 (**C**) and cyclo-oxygenase 2 (**D**) in the retinal tissues of all groups. ns: not significant; **p<0.01 compared with the oxygen-induced retinopathy (OIR)group; ***p<0.001 compared with the OIR group.

of HRCEC culture, pairwise comparisons between groups with high-glucose + different concentrations of UA groups (5, 10, 20, 40 μmol/l) showed that the inhibition rate of the HRCECs increased with an increased concentration and reflected a statistically significant difference (p<0.05). After intervention of the same concentration of UA, the inhibition rate of the HRCECs was increased along with the drug intervention time; the difference was statistically significant (p<0.05; Table 2 and Table 3).

Effect of different concentrations of ursolic acid on the protein expression of vascular endothelial growth factor, matrix metalloproteinase-2, matrix metalloproteinase-9 and

Table 2. Effects of different concentrations of UA on HRCECs cell proliferation in high glucose environment (n=5).

Group	A490 value		
	24 h	48 h	72 h
The TN group	0.4029 ± 0.139	0.4269 ± 0.007	0.4539 ± 0.005
The TH group	0.6291 ± 0.006*	0.6583 ± 0.005*	0.6947 ± 0.004*
The T1 group	0.5689 ± 0.006#	0.5472 ± 0.005#	0.5243 ± 0.006#
The T2 group	0.4726 ± 0.009#	0.4379 ± 0.004#	0.4054 ± 0.008#
The T3 group	0.4278 ± 0.014#	0.4012 ± 0.007#	0.3647 ± 0.008#
The T4 group	0.3969 ± 0.007#	0.3679 ± 0.005#	0.3168 ± 0.005#

Note: compared with TN group, *p<0.05; Compared with TH group, #p<0.05. UA: ursolic acid; HRCECs: Human Retinal Capillary Endothelial Cells. TN group: normal glucose (glucose concentration, 5.5 mmol/l); TH group: high glucose (glucose concentration, 25 mmol/l); T1 group: high glucose + 5 μmol/l UA; T2 group: high glucose + 10 μmol/l UA; T3 group: high glucose + 20 μmol/L UA; T4 group: high glucose + 40 μmol/l UA.

cyclo-oxygenase-2 in human retinal capillary endothelial cells in a high-glucose environment: The protein expression of VEGF, MMP-2, MMP-9 and COX-2 in different HRCEC groups was determined by protein immunoblot (western blot) as follows:

(1) After HRCEC cultures were performed simultaneously, the protein expression of VEGF, MMP-2, MMP-9 and COX-2 in HRCECs was higher in the high-glucose group than in the normal glucose group; analysis results of the gray band protein value were significantly different (p<0.05; Figure 5A).

(2) After the same culture time, pairwise comparisons between the high-glucose and different-concentration (5, 10, 20, 40 μmol/l) UA groups showed that the expression of VEGF, MMP-2, MMP-9 and COX-2 in HRCECs decreased with increased concentration of UA; the differences were statistically significant (p<0.05). With the extension of UA intervention time, there was a gradual decrease in the expression levels of VEGF, MMP-2, MMP-9 and COX-2. Specifically, the levels observed were lower in the 72-h group than in the 48-h group, and the 48-h group exhibited lower levels compared with the 24-h group; the differences were statistically significant (p<0.05; Figure 5B–D).

Effect of different concentrations of ursolic acid on the messenger ribonucleic acid levels of vascular endothelial growth factor, matrix metalloproteinase-2, matrix metalloproteinase-9 and cyclo-oxygenase-2 in human retinal capillary endothelial cells in a high-glucose environment: Real-time PCR was conducted to detect the mRNA levels of VEGF, MMP-2, MMP-9 and COX-2 in the HRCECs of different groups. Following simultaneous HRCEC culture, the mRNA levels of VEGF, MMP-2, MMP-9 and COX-2 were higher in the high-glucose group than in the normal glucose group; the differences were statistically significant (p<0.05). With the same culture time, pairwise comparisons between groups with high-glucose + different concentrations (5, 10, 20, 40 μmol/L) of UA showed that the mRNA levels of VEGF, MMP-2, MMP-9 and COX-2 in HRCECs decreased with an increased concentration of UA; the differences were statistically significant (p<0.05). mRNA levels of HRCECs, MMP-2, MMP-9 and COX-2 decreased with prolonged drug

Table 3. Inhibition rate of different concentrations of UA on HRCECs cells in high glucose environment.

Group	24 h	48 h	72 h
The TH group	-	-	-
The T1 group	9.6%	13.8%	16.9%
The T2 group	24.9%	33.9%	40.7%
The T3 group	32.1%	38.6%	47.0%
The T4 group	37.0%	43.3%	52.9%

Note: The calculation formula of inhibition rate is: (1 - OD value of experimental group/OD value of TH group) × 100%; TN group: normal glucose (glucose concentration, 5.5 mmol/l); TH group: high glucose (glucose concentration, 25 mmol/l); T1 group: high glucose + 5 μmol/l UA; T2 group: high glucose + 10 μmol/l UA; T3 group: high glucose + 20 μmol/l UA; T4 group: high glucose + 40 μmol/l UA.

intervention; the differences were statistically significant ($p<0.05$; Figure 6).

DISCUSSION

Terry et al. first reported ROP in 1942 [12]. In the early 1950s, several scholars suggested that ROP may be associated with the toxic side effects of clinical high-concentration oxygen therapy [13,14]; subsequent animal experiments have confirmed this view, thus establishing a series of animal models of OIR [15]. The OIR model is able to simulate the entire pathological change process of RNV to the greatest extent. UA has various biologic effects, including antitumor, antioxidation, antineovascular, antivirus and antibacterial effects [16]. It inhibits neovascularization by suppressing vascular endothelial cell migration and tubular production, as well as by reducing the expression of angiogenic factors [17,18].

Kanjoormana et al. [19] confirmed that the expression levels of the proinflammatory factors VEGF and neuraminidase decreased significantly following UA intervention in melanocytomas in mice. In the results of their study the protein expression of MMP-2 and MMP-9 decreased,

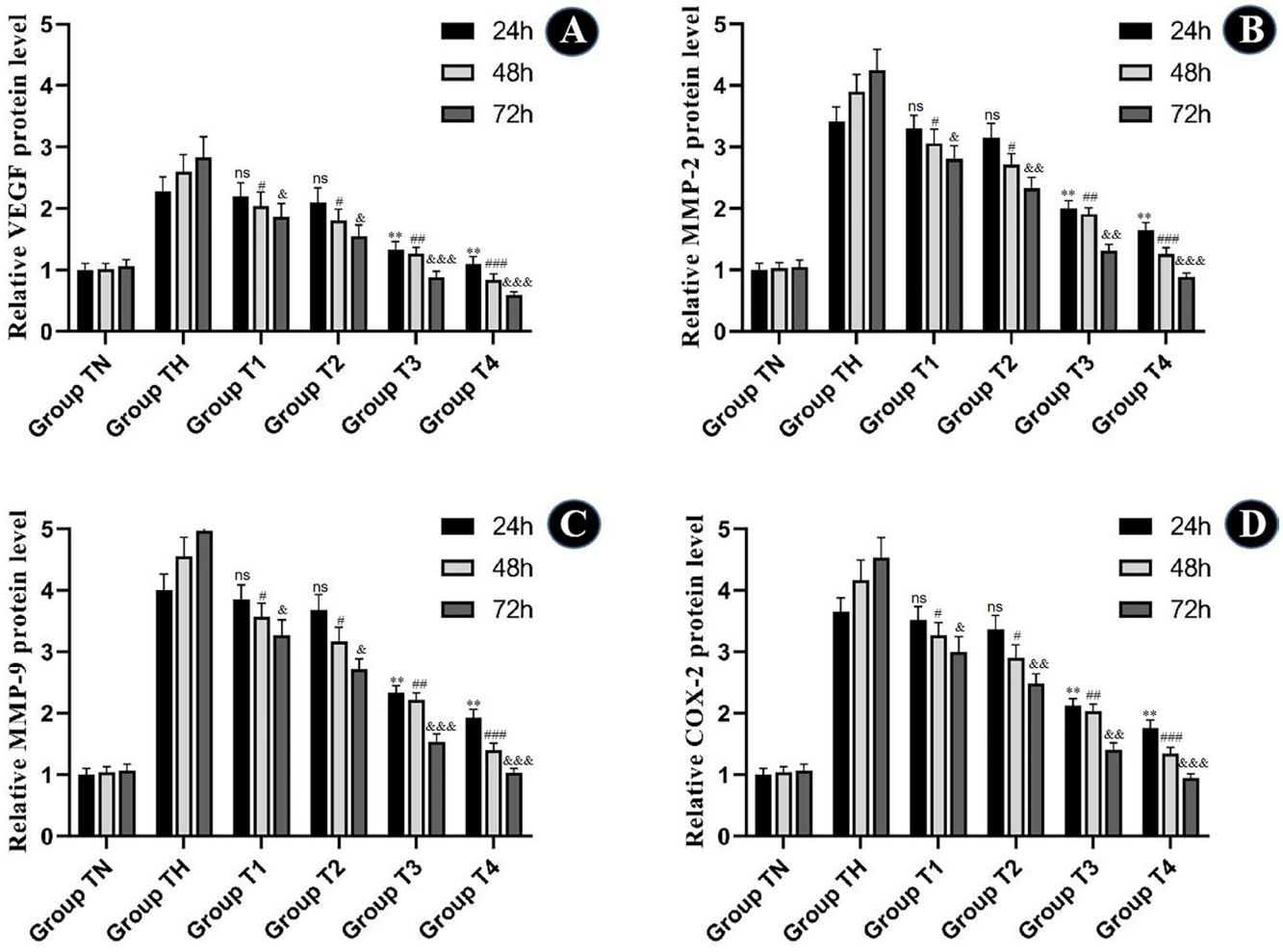

Figure 5. The relative protein level in each group. Expression levels of vascular endothelial growth factor (**A**), matrix metalloproteinase 2 (**B**), matrix metalloproteinase 9 (**C**) and cyclo-oxygenase 2 (**D**) proteins of human retinal capillary endothelial cells in different groups. ns: not significant; **p<0.01 compared with TH group 24 h; #p<0.05, ##p<0.01, ###p<0.001 compared with TH group 48 h; &p<0.05, &&p<0.01, &&&p<0.001 compared with TH group 72 h. TN group: normal glucose (glucose concentration, 5.5 mmol/l); TH group: high glucose (glucose concentration, 25 mmol/l); T1 group: high glucose + 5 μmol/l ursolic acid (UA); T2 group: high glucose + 10 μmol/l UA; T3 group: high glucose + 20 μmol/l UA; T4 group: high glucose + 40 μmol/l UA.

whereas the mRNA of VEGF and induced nitric oxide synthase decreased. Zhang et al. [20] found that UA induced the apoptosis of SGC-7901 in a human gastric cancer cell line by inhibiting the expression of COX-2 and subsequently reducing the synthesis of prostaglandin E2. VEGF, MMP-2, MMP-9 and COX-2 play important roles in the RNV process [21-25]. Therefore, based on the properties of UA, they can be used for the treatment of hypoxia-induced retinopathy, such as ROP. However, more studies should be conducted to verify this result.

Lucentis is an FDA-approved antiangiogenic drug [26]. All isoforms of Lucentis and VEGF-A have a strong affinity. The main mechanism of inhibiting neovascularization is competitive binding of the VEGF receptor on the endothelial cell surface, blocking the binding of VEGF to its receptor and resulting in the loss of VEGF activity rather than quantitative reduction [27,28]. Therefore, the anti-VEGF antibody Lucentis, which has a largely clear clinical effect and mechanism, was selected for UA in the positive control group to explore a controlled study on the regulation of RNV generation in the retina of mice with OIR.

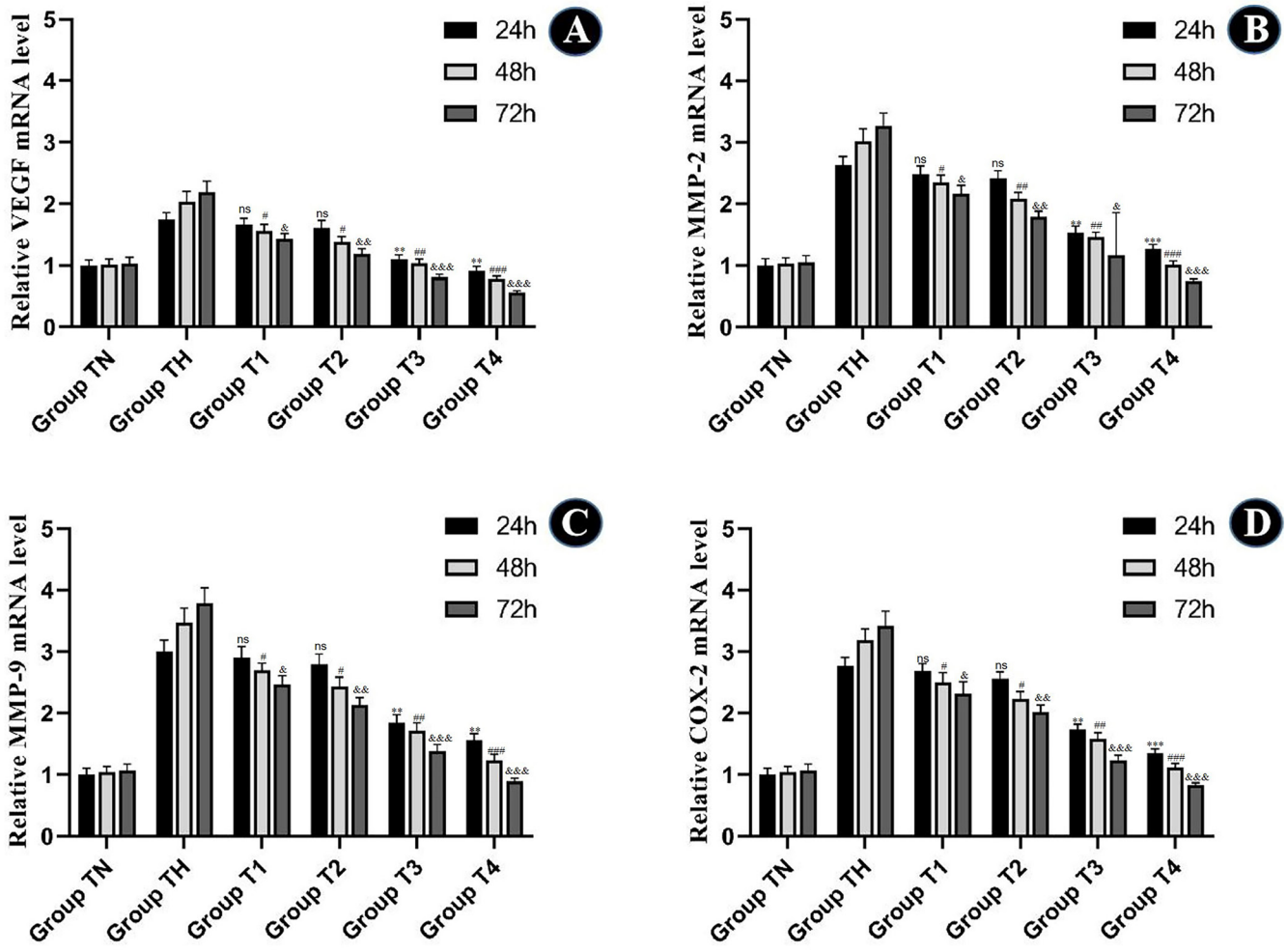

Figure 6. The relative mRNA level in each group. Expression levels of vascular endothelial growth factor (**A**), matrix metalloproteinase 2 (**B**), matrix metalloproteinase 9 (**C**) and cyclo-oxygenase 2 (**D**) mRNA in different groups of human retinal capillary endothelial cells. ns: not significant; **p<0.01, ***p<0.001 compared with TH group 24 h; #p<0.05, ##p<0.01, ###p<0.001 compared with TH group 48 h; &p<0.05, &&p<0.01, &&&p<0.001 compared with TH group 72 h. TN group: normal glucose (glucose concentration, 5.5 mmol/l); TH group: high glucose (glucose concentration, 25 mmol/l); T1 group: high glucose + 5 μmol/l ursolic acid (UA); T2 group: high glucose + 10 μmol/l UA; T3 group: high glucose + 20 μmol/l UA; T4 group: high glucose + 40 μmol/l UA.

Recent studies confirmed that retinal astrocytes are also affected in such diseases and are closely associated with dysplastic pathological neovascularization. Glial cell dysfunction has also been previously reported in the hypoxic retina [29]. Astrocytes and Müller cells may play a role in the progression of OIR; that is, they potentially contribute to regulating oxygen concentrations and environmental conditions within the retina, influencing vascular development. Given the connection between abnormal retinal vascular development and OIR, glial cells may be involved in retinal vascular system development and stability through aspects such as cytokines, growth factors and intercellular communication. Thus, protecting astrocytes is also key in the treatment of RNV diseases. Dorrell et al. [30] revealed that loss of astrocytes directly correlates with the development of pathological neovascularization in a mouse model of OIR. The present study confirmed that, compared with normal controls, the heteromorphosis of retinal astrocytes was evident in addition to RNV in mice with OIR. These results are in line with those reported by Dorrell et al. [30]. In the hypoxic phase, UA morphologically inhibited RNV generation in mice with OIR, reduced astrocyte damage and supported astrocytes in forming their normal astral/dendritic shape. The authors of the present study confirm that UA may inhibit OIR in mice by protecting astrocytes.

VEGF, MMP-2, MMP-9 and COX-2 are all closely related to the generation of RNV; therefore, inhibiting the expression of the above factors can effectively reduce the risk of RNV. Arrigo et al. [31] revealed that VEGF-targeting drugs were useful for the treatment of RNV in DR, and Yu et al. [32] found that overexpression of miR-203 suppressed angiogenesis in mice with pathological RNV disease via inhibiting the expression of K_i-67, MMP-2, MMP-9 and VEGF. In the present study, the results in each group suggest that the protein expression and mRNA levels of VEGF, MMP-2, MMP-9 and COX-2 factors were significantly higher in the OIR and PBS groups than in the normal group. Following intravitreal UA and Lucentis intervention, VEGF decreased significantly. There was no statistically significant difference between the two groups, but the protein expression and mRNA levels of MMP-2, MMP-9 and COX-2 factors decreased significantly in the UA group; no significant change was observed in the Lucentis group. These results aligned with those of Arrigo et al. [31] and Yu et al. [32]. Therefore, it is speculated that UA inhibits RNV generation by reducing the expression of VEGF, MMP-2, MMP-9 and COX-2, whereas Lucentis inhibits RNV generation only by limiting VEGF factor expression, with no significant effect on factors such as MMP-2, MMP-9 and COX-2. Lucentis is a single anti-VEGF drug and can only inhibit the formation of new blood vessels. In the context of the present research, UA has emerged as a more cost-effective alternative to Lucentis, exhibiting a synergistic effect on astrocytes and thus underscoring its promising clinical therapeutic significance.

In this study, UA was used to intervene in in vitro HRCEC culturing in a high-glucose environment to observe its possible therapeutic effect on DR. The relationship between DR and oxygen-induced RNV lies in the common underlying process of neovascularization. In both cases, damaged blood vessels trigger the release of growth factors that promote the creation of new blood vessels. These new blood vessels are abnormal and fragile, making them prone to leakage and bleeding. In DR, this process is driven by chronic high blood glucose levels damaging retinal blood vessels. In OIR, it is triggered by the disruption of normal retinal vascular development due to high levels of oxygen exposure. The experimental results suggest that the protein expression and mRNA levels of VEGF, MMP-2, MMP-9 and COX-2 were higher in the high-glucose groups than in the normal glucose groups during the same period. The protein expression and mRNA levels of VEGF, MMP-2, MMP-9 and COX-2 in HRCECs decreased with an increased concentration of UA and prolonged drug intervention. This suggests that UA has inhibitory effects on HRCEC proliferation in vitro in a high-glucose model and in a time–concentration-dependent manner.

This study employed the mouse OIR model, which effectively simulates RNV in humans. However, structural and physiologic differences between mouse and human retinas may limit the direct extrapolation of results. Notably, the retinal response to hypoxia involves not only endothelial cells but also astrocytes and Müller cells. These cells play critical roles in regulating oxygen levels and secreting cytokines and growth factors, thereby significantly contributing to hypoxia-induced angiogenesis. Compared with isolated endothelial cell experiments, the OIR model offers a more comprehensive perspective on cellular interactions [33,34]. Additionally, glucose and hypoxia influence retinal endothelial cell proliferation through distinct mechanisms. Glucose primarily promotes pathological angiogenesis by activating protein kinase C, increasing oxidative stress and elevating inflammatory factors, such as tumor necrosis factor alpha and interleukin-6 [35]. Hypoxia, on the other hand, induces VEGF expression via hypoxia-inducible factor-1 alpha, facilitating endothelial cell migration and angiogenesis [36]. These differences highlight the unique drivers and cellular signaling networks in DR and hypoxia-induced RNV. High glucose is a key pathogenic factor in DR, which leads to pathological changes such as retinal vascular endothelial cell dysfunction,

exacerbated inflammatory response and neovascularization. Therefore, we modeled the pathological environment of DR by high-glucose treatment and observed the protective effect of UA on HRCECs in this environment. We are also aware of the importance of hypoxia in the OIR model and plan to incorporate hypoxia treatment into the experimental design in subsequent studies to assess the role of UA in the pathological processes associated with retinopathy more comprehensively. However, a limitation of this study lies in the small sample size, which is common in animal research. Additionally, it is essential to exercise caution when extrapolating findings from animal models to human clinical applications, acknowledging inherent physiologic and biologic differences.

In conclusion, the mechanism of UA to effectively inhibit oxygen-induced RNV generation and HRCEC proliferation in vitro in high-glucose models may be reducing the expression of VEGF, preventing the migration of vascular endothelial cells, reducing prostaglandin E2, reducing the expression of MMP-2 and MMP-9, promoting vascular endothelial cell apoptosis and reducing extracellular matrix degradation, whereas UA protects the vascular ‘base bed’ astrocytes. Therefore, multitarget UA inhibition of RNV has broad prospects in clinical application.

ACKNOWLEDGMENTS

Ethics approval and consent to participate: The experimental protocol was approved by the Animal Experimentation Ethics Committee of Shanxi Aier Eye Hospital. Experimental animals underwent all procedures under anesthesia, and every effort was made to minimize their pain, suffering, and death. This study was conducted in accordance with the principles on ethical animal research outlined in the Basel Declaration and the ethical guidelines by the International Council for Laboratory Animal Science (ICLAS). This study was conducted in accordance with NC3Rs ARRIVE guidelines. Availability of data and materials: All data generated or analyzed during this study are included in this article. Competing interest: All of the authors had no personal, financial, commercial, or academic conflicts of interest separately. Funding: 1. Natural Science Foundation of Shanxi Province: Study on regulation of VEGFR-2/3 dependent retinal neovascularization by proanthocyanidins through Activation of AIP1 (202403021211119). 2. Taiyuan "Six batch" special action research project (Key project): "Research on the mechanism of DSCR1 Regulating CaN signaling Pathway on retinal neovascularization" (Z2024010). 3. Shanxi Provincial Administration of Traditional Chinese Medicine Research Project: "The effect of curcumin extracts on oxygen-induced Retinal vascular Proliferation and oxidative Stress" (2022ZYYC118). 4. Guiding Project of Aier Eye Research Foundation: "Study on Regulation of retinal neovascularization by Proanthocyanidins through VEGFR-2/3 Dependent Signaling Pathway" (AGK2301D15). Author Contributions: (I) Conception and design: Yang L, Yang F and Zhang WL; (II) Administrative support: Gao Y, Wang YH and Chen P; (III) Provision of study materials or patients: Qiang Su and Du SF; (IV) Collection and assembly of data: Shi JH and Li R; (V) Data analysis and interpretation:Wang P and Liu XY. Dr. Lu Yang (yl16082022@163.com), Dr. Weiliang Zhang (zwlfracure@126.com) and Dr. Qiang Su (50536224@qq.com) are co-corresponding authors for this paper.

REFERENCES

1. Lee YM, Lee YR, Kim CS, Jo K, Sohn E, Kim JS, Kim J. Effect of Guibi-Tang, a Traditional Herbal Formula, on Retinal Neovascularization in a Mouse Model of Proliferative Retinopathy. Int J Mol Sci 2015; 16:29900-10. [PMID: 26694358].
2. Mammadzada P, Bayle J, Gudmundsson J, Kvanta A, André H. Identification of Diagnostic and Prognostic microRNAs for Recurrent Vitreous Hemorrhage in Patients with Proliferative Diabetic Retinopathy. J Clin Med 2019; 8:2217-[PMID: 31847440].
3. Hu Y, Lu X, Xu Y, Lu L, Yu S, Cheng Q, Yang B, Tsui CK, Ye D, Huang J, Liang X. Salubrinal attenuated retinal neovascularization by inhibiting CHOP-HIF1α-VEGF pathways. Oncotarget 2017; 8:77219-32. [PMID: 29100382].
4. Madonna R, Giovannelli G, Confalone P, Renna FV, Geng YJ, De Caterina R. High glucose-induced hyperosmolarity contributes to COX-2 expression and angiogenesis: implications for diabetic retinopathy. Cardiovasc Diabetol 2016; 15:18-[PMID: 26822858].
5. Lee YK, Lim J, Yoon SY, Joo JC, Park SJ, Park YJ. Promotion of Cell Death in Cisplatin-Resistant Ovarian Cancer Cells through KDM1B-DCLRE1B Modulation. Int J Mol Sci 2019; 20:2443-[PMID: 31108893].
6. Mu H, Liu H, Zhang J, Huang J, Zhu C, Lu Y, Shi Y, Wang Y. Ursolic acid prevents doxorubicin-induced cardiac toxicity in mice through eNOS activation and inhibition of eNOS uncoupling. J Cell Mol Med 2019; 23:2174-83. [PMID: 30609217].
7. Connor KM, Krah NM, Dennison RJ, Aderman CM, Chen J, Guerin KI, Sapieha P, Stahl A, Willett KL, Smith LE. Quantification of oxygen-induced retinopathy in the mouse: a model of vessel loss, vessel regrowth and pathological angiogenesis. Nat Protoc 2009; 4:1565-73. [PMID: 19816419].
8. Smith LE, Wesolowski E, McLellan A, Kostyk SK, D’Amato R, Sullivan R, D’Amore PA. Oxygen-induced retinopathy in the mouse. Invest Ophthalmol Vis Sci 1994; 35:101-11. [PMID: 7507904].
9. García-Quintanilla L, Luaces-Rodríguez A, Gil-Martínez M, Mondelo-García C, Maroñas O, Mangas-Sanjuan V,

González-Barcia M, Zarra-Ferro I, Aguiar P, Otero-Espinar FJ, Fernández-Ferreiro A. Pharmacokinetics of Intravitreal Anti-VEGF Drugs in Age-Related Macular Degeneration. Pharmaceutics 2019; 11:365-[PMID: 31370346].

10. Li B, Tang SB, Hu J, Gao Y, Zhang G, Lin SF, Chen JH, Li BJ. Protective effects of transcription factor HESR1 on retinal vasculature. Microvasc Res 2006; 72:146-52. [PMID: 17028039].

11. Shen H, Gong Q, Zhang J, Wang H, Qiu Q, Zhang J, Luo D. TRIM46 aggravated high glucose-induced hyper permeability and inflammatory response in human retinal capillary endothelial cells by promoting IκBα ubiquitination. Eye Vis (Lond) 2022; 9:35-[PMID: 36064447].

12. Terry TL. Extreme prematurity and fibroblastic overgrowth of persistent vascular sheath behind each crystalline lens: I. Preliminary report. Am J Ophthalmol 1942; 25:203-4. [PMID: 30055814].

13. Scott A, Powner MB, Fruttiger M. Quantification of vascular tortuosity as an early outcome measure in oxygen induced retinopathy (OIR). Exp Eye Res 2014; 120:55-60. [PMID: 24418725].

14. Hartnett ME. The effects of oxygen stresses on the development of features of severe retinopathy of prematurity: knowledge from the 50/10 OIR model. Doc Ophthalmol 2010; 120:25-39. [PMID: 19639355].

15. Ricci B, Lepore D, Zonghi E, Calogero G. Oxygen-induced retinopathy in the newborn rat: a scoring system for the evaluation of retinal vascular changes. Scoring system for OIR in the rat. Doc Ophthalmol 1990-1991; 76:241-9. [PMID: 2103526].

16. Kuttan G, Pratheeshkumar P, Manu KA, Kuttan R. Inhibition of tumor progression by naturally occurring terpenoids. Pharm Biol 2011; 49:995-1007. [PMID: 21936626].

17. Kurek A, Grudniak AM, Szwed M, Klicka A, Samluk L, Wolska KI, Janiszowska W, Popowska M. Oleanolic acid and ursolic acid affect peptidoglycan metabolism in Listeria monocytogenes. Antonie Van Leeuwenhoek 2010; 97:61-8. [PMID: 19894138].

18. Pinon A, Limami Y, Micallef L, Cook-Moreau J, Liagre B, Delage C, Duval RE, Simon A. A novel form of melanoma apoptosis resistance: melanogenesis up-regulation in apoptotic B16-F0 cells delays ursolic acid-triggered cell death. Exp Cell Res 2011; 317:1669-76. [PMID: 21565187].

19. Kanjoormana M, Kuttan G. Antiangiogenic activity of ursolic acid. Integr Cancer Ther 2010; 9:224-35. [PMID: 20462855].

20. Zhang YY, Deng T, Hu ZF, Zhang QP, Zhang J, Jiang H. [Mechanisms of inhibiting proliferation and inducing apoptosis of human gastric cancer cell line SGC7901 by ursolic acid] Ai Zheng 2006; 25:432-7. [PMID: 16613675].

21. Zheng L, Gong B, Hatala DA, Kern TS. Retinal ischemia and reperfusion causes capillary degeneration: similarities to diabetes. Invest Ophthalmol Vis Sci 2007; 48:361-7. [PMID: 17197555].

22. Hu JF, Di ZQ, Huo X, Shen XP. Correlation between retinal vascular endothelial growth factor and retinal neovascularization in mice. Yaowu Pingjia Yanjiu 2012; 35:250-2. .

23. Bekowitz BA, Roberts R, Luan H, Peysakhov J, Knoerzer DL, Connor JR. et a1. Drug intervention can correct subnormal retinal oxygenation response in experimental diabetic retinophathyInvest Ophthalmol Vis Sci 2005; 46:2954-60. [PMID: 16043871].

24. Liu NN, Zhao N, Liu LM, Chen L, Cai N. Cyclooxygenase 2 and survivin expression in retinal neovascularization. Int J Ophthalmol 2013; 13:46-8. .

25. Li J, Hao YH. Expressions of COX-2,VEGF and MMP-2 in experimental choroidal neovascularization model. Chinese Ophthalmic Research. 2010; 28:836-40. .

26. Matsubara JA, Tian Y, Cui JZ, Zeglinski MR, Hiroyasu S, Turner CT, Granville DJ. Retinal Distribution and Extracellular Activity of Granzyme B: A Serine Protease That Degrades Retinal Pigment Epithelial Tight Junctions and Extracellular Matrix Proteins. Front Immunol 2020; 11:574-[PMID: 32318066].

27. Wang Y, Da G, Li H, Zheng Y. Avastin exhibits therapeutic effects on collagen-induced arthritis in rat model. Inflammation 2013; 36:1460-7. [PMID: 23851616].

28. Cruess AF, Giacomantonio N. Cardiac issues of noncardiac drugs: the rising story of avastin in age-related macular degeneration. Ophthalmologica 2014; 231:75-9. [PMID: 24217407].

29. Morfoisse F, Kuchnio A, Frainay C, Gomez-Brouchet A, Delisle MB, Marzi S, Helfer AC, Hantelys F, Pujol F, Guillermet-Guibert J, Bousquet C, Dewerchin M, Pyronnet S, Prats AC, Carmeliet P, Garmy-Susini B. Hypoxia induces VEGF-C expression in metastatic tumor cells via a HIF-1α-independent translation-mediated mechanism. Cell Rep 2014; 6:155-67. [PMID: 24388748].

30. Dorrell MI, Aguilar E, Jacobson R, Trauger SA, Friedlander J, Siuzdak G, Friedlander M. Maintaining retinal astrocytes normalizes revascularization and prevents vascular pathology associated with oxygen-induced retinopathy. Glia 2010; 58:43-54. [PMID: 19544395].

31. Arrigo A, Aragona E, Bandello F. VEGF-targeting drugs for the treatment of retinal neovascularization in diabetic retinopathy. Ann Med 2022; 54:1089-111. [PMID: 35451900].

32. Yu L, Wu S, Che S, Wu Y, Han N. Inhibitory role of miR-203 in the angiogenesis of mice with pathological retinal neovascularization disease through downregulation of SNAI2. Cell Signal 2020; 71:109570[PMID: 32084532].

33. Carmeliet P, Jain RK. Molecular mechanisms and clinical applications of angiogenesis. Nature 2011; 473:298-307. [PMID: 21593862].

34. Dorrell MI, Friedlander M. Mechanisms of endothelial cell guidance and vascular patterning in the developing mouse retina. Prog Retin Eye Res 2006; 25:277-95. [PMID: 16515881].

35. Brownlee M. Biochemistry and molecular cell biology of diabetic complications. Nature 2001; 414:813-20. [PMID: 11742414].

36. Semenza GL. Hypoxia-inducible factors in physiology and medicine. Cell 2012; 148:399-408. [PMID: 22304911].